Clim. Past Discuss., 9, 119–142, 2013
www.clim-past-discuss.net/9/119/2013/
doi:10.5194/cpd-9-119-2013

Climate of the Past Discussions

Abrupt shifts of the Sahara-Sahel boundary during Heinrich Stadials

J. A. Collins[1], A. Govin[1], S. Mulitza[1], D. Heslop[2], M. Zabel[1], J. Hartmann[3], U. Röhl[1], and G. Wefer[1]

[1]MARUM – Center for Marine Environmental Sciences and Faculty of Geosciences, University of Bremen, 28359 Bremen, Germany
[2]Research School of Earth Sciences, The Australian National University, Canberra ACT 0200, Australia
[3]Institute for Biogeochemistry and Marine Chemistry, University of Hamburg, Bundesstraße 55, 20146 Hamburg, Germany

Received: 14 December 2012 – Accepted: 20 December 2012 – Published: 4 January 2013

Correspondence to: J. A. Collins (jcollins@marum.de)

Published by Copernicus Publications on behalf of the European Geosciences Union.

Abstract

Relict dune fields that are found at 14° N in the modern-day African Sahel are testament to equatorward expansions of the Sahara desert during the late Pleistocene. However, difficulties of dating dune formation mean that abrupt millennial-scale climate events are not always resolved in these records. High-resolution marine core studies have identified Heinrich Stadials as the dustiest periods of the last glacial, although no studies have mapped the spatio-temporal evolution of dust export from West Africa. We use the major-element composition of four marine sediment cores to reconstruct the spatial extent of Saharan-dust versus river-sediment input to the continental margin from West Africa over the last 60 ka. This allows us to map the position of the sediment composition corresponding to the Sahara-Sahel boundary. Our records indicate that the Sahara-Sahel boundary reached its most southerly position (13° N) during Heinrich Stadials, suggesting that these were the periods when the sand dunes formed at 14° N on the continent, rather than at the Last Glacial Maximum. We find that SSB position was closely linked to North Atlantic sea surface temperatures, which during Heinrich Stadials triggered abrupt increases of aridity and wind strength in the Sahel, exposing new dust sources. This result illustrates the influence of the Atlantic meridional overturning circulation on the southerly extent of the Sahara desert and has implications for global atmospheric dust loading.

1 Introduction

Understanding the extent and causes of abrupt millennial-timescale expansions of the Sahara desert is important for the populations of the Sahel region, where dune encroachment causes major problems (FAO, 2010). In addition, constraining the size of the Saharan dust plume is important for determining the role of dust as a climate feedback (e.g. Rosenfeld et al., 2001).

CPD
9, 119–142, 2013

Relict dune fields in the modern-day Sahel indicate that during the late Pleistocene, the Sahara desert during was extended further south than today (Grove, 1958; Talbot, 1980). These relicts had previously migrated equatorwards and are now held in place by vegetation (Sarnthein and Diester-Haass, 1977). They are found throughout the Sahel (Fig. 1a) as far south as ~ 14° N (Grove, 1958; Michel, 1973). This is ~ 5° south of the modern-day boundary of dune formation (at ~ 19° N in the Western Sahara), which we define as the Sahara-Sahel boundary (SSB; Fig. 1a) after e.g. Sarnthein and Diester-Haass (1977) and Kocurek et al. (1991). It has been challenging, however, to determine the timing of dune formation due to re-mobilisation of dunes (Kocurek et al., 1991). Nonetheless, certain phases have been identified (Talbot, 1980), including an "Early" phase (> 40 ka; Servant, 1983), a more extensive "Ogolian" phase (24–12 ka; Michel, 1973; Servant, 1983; Lancaster et al., 2002), and a "Late" phase following the mid-Holocene (< 5 cal ka BP; Swezey, 2001).

Continental pollen records have also been used to reconstruct the continental SSB evolution and infer an equatorward displacement of ~ 5° latitude at the Last Glacial Maximum (LGM; Dupont and Hooghiemstra, 1989; Lézine, 1989). However, these records have a relatively low temporal resolution and do not resolve abrupt millennial-scale climate changes. In addition, marine sediment mapping studies have only focussed on the LGM (Sarnthein, et al., 1981; Grousset et al., 1998; Hooghiemstra et al., 2006). These studies suggested a stronger dust plume at the LGM compared to today but a stable latitudinal position of the desert belt.

Marine sediment cores can provide high-resolution and continuous records of material exported from the continent. Cores from the tropical NE Atlantic between 21° N and 12° N (e.g. Jullien et al., 2007; Mulitza et al., 2008; Tjallingii et al., 2008; Itambi et al., 2009; Zarriess et al., 2011) indicate strong increases in dust export from West Africa during Dansgaard-Oeschger (D-O) stadials associated with Heinrich Events (Heinrich Stadials; HS). However, the use of different methods prevents a direct comparison of the relative magnitude of variations at each site and thus prevents mapping of the spatial extent of the Sahara desert during these millennial-timescale events.

Using major-element composition of sediments from four marine cores spanning the Sahara to the Guinea coast (21° N–9° N) we are able to quantify the relative contribution of Saharan dust versus river-sediment to the continental shelf. We mapped the spatial (North–South) evolution of dust versus river input over the last 60 ka. Comparison with continental records of dune formation supports our interpretation that the sedimentary records reflect the position of the continental SSB over the last 60 ka.

2 Setting

The continental margin off West Africa receives terrigenous material in the form of two sources: river-suspended sediment and windblown dust. Rivers originate from the humid, high-altitude Fouta Djallon region and enter the ocean between 16° N–5° N (Fig. 1a). The soils of the Fouta Djallon are deeply chemically weathered and are composed mainly of clays (Driessen et al., 2001). As such, river-suspended sediment is relatively enriched in Fe and Al (Table S1 in the Supplement).

The main source of windblown dust is the Sahara, with a small contribution from the Sahel (Goudie and Middleton, 2001). Most of the dust delivered to the West African margin is blown from the Mali-Mauritania region (Fig. 1b) by the winter North-East trade winds (Sarnthein et al., 1981; Bory and Newton, 2000). Some dust is also entrained into the Saharan Air Layer by convective summer storms and travels further, some reaching the Caribbean (Prospero et al., 1981). Dust originates from arid regions, which, for the major source regions, have remained relatively arid during most of the Pleistocene (deMenocal, 1995). Therefore, compared to river-sediment, dust is relatively enriched in Si and K (Table S1 in the Supplement). At the coast, the dust plume spans approximately 25° N–15° N, centred at ~ 20° N (Fig. 1b). As such, this results in a Si-rich dust source located to the north of the Al- and Fe-rich fluvial source region. In these samples, there is little difference between river sediment load and dust in terms of their proportion of Ti.

CPD
9, 119–142, 2013

The North–South gradient between the two sources of material is reflected in the major-element composition of continental margin surface sediments (Govin et al., 2012; Fig. 1c), with the lowest Al/Si ratios in the northernmost, dust-dominated part of our study region.

3 Methods

We use 4 sediment cores (Table 1) spanning from 21° N to 9° N off West Africa (Fig. 1) covering the gradient between dust and river sources. Sediment core chronology is based on published age models (see Table 1 for references) using both radiocarbon and benthic foraminiferal $\delta^{18}O$ correlation.

Sediment major-element composition was measured using the Avaatech X-Ray Fluorescence Core Scanner at MARUM, University of Bremen (Cores 1 and 2; Bloemsma et al., 2012 and Core 4; this study) and at AWI, Bremerhaven (Core 3; Zarriess and Mackensen, 2010; Zarriess et al., 2011). XRF scanner elemental intensities were calibrated to elemental concentrations (Weltje and Tjallingii, 2008) by regression with at least 50 discrete powder samples from each core (Core 1; Bloemsma et al., 2012; Core 2; Mulitza et al., 2008; Cores 3 and 4; this study), which were quantified using EDP-XRF spectroscopy at the MARUM, University of Bremen. The robustness of the calibration is indicated as the fit of the calibrated scanner data with the discrete powder samples (Fig. S1 in the Supplement).

Commonly, major-element data are presented as elemental ratios (e.g. Mulitza et al., 2008; Zarriess et al., 2011). Rather than interpreting elemental ratios, we directly quantify the major element data in terms of the relative proportion of Saharan dust, river-suspended material and marine-derived material by using an end-member unmixing analysis using. Details of this analysis are given in Mulitza et al. (2010). Briefly, representative "dust" and "river" end-member major-element compositions were estimated using a bootstrap with replacement routine (500 iterations) based on the relative proportions of Al, Si, Fe, K, Ti and Ca from 28 Sahara-Sahel dust and soil samples and 10

Senegal River suspension samples (Table S1 in the Supplement). The composition of the marine component (Ca and Si; Table S1 in the Supplement) was estimated based on biogenic silica content (Collins et al., 2011) and the measured Ca concentration, and was held constant downcore (after Mulitza et al., 2010). The contribution of Si from biogenic opal is low (< 3.5 wt% SiO_2) and downcore variations, between major climate regimes (e.g. modern-day, LGM and HS1) are small. Error on the marine end-member composition (Table S1 in the Supplement) was nonetheless integrated into the unmixing analysis and propagated into the final uncertainty on the dust% estimates. We represent the data as dust%, where dust% = $100 \times$ dust/(river + dust). Dust% is the median value of the 500 bootstrap iterations and uncertainty is represented as non-parametric 68 % confidence intervals (16th and 84th percentiles). Because of the difficulty of constraining the sedimentation rate of each millennial-scale event (Just et al., 2012) we do not estimate dust accumulation rates.

Dust% is closely correlated to the Al/Si ratios (Fig. 1c) because these elements differ most strongly between the dust and river end-members (Table S1 in the Supplement). Downcore Al/Si ratios are also given in Fig. S2 in the Supplement for comparison with our dust% data.

To determine the modern-day dust% value in the sediment at the latitude of the Sahara-Sahel boundary (19° N), we performed a robust linear regression between latitude and dust% for the surface sediments between 26° N and 3° N (Govin et al., 2012) and the late Holocene sections (mean of core-top to 3 ka) of our cores (Fig. 1c). Uncertainty is represented as 68 % confidence intervals on the regression.

To determine the position of the SSB over time, we linearly interpolated each of the four sediment-core dust% timeseries every 250 yr. For each timestep, we performed a robust linear regression between dust% and latitude and solved the equation to calculate the latitude corresponding to the modern-day SSB dust% value. Propagated uncertainties include: uncertainty on the end-member composition, uncertainty on the modern-day SSB dust% and uncertainty on the regression for the past timesteps (based on 68 % confidence intervals on the regression). Examples of the linear regression for timesteps from a range of climate states are given (Fig. S3 in the Supplement).

4 Results

For the surface sediments and late Holocene section of the sediment cores, dust% values decrease from north to south, e.g. from 51 % at Core 1 (21° N) to 3 % at Core 4 (9° N; Fig. 1c). At the latitude of the modern-day SSB (19° N), the regression between latitude and dust yields a dust% value of 43 % ± 9 % (Fig. 1c).

Dust% values in Cores 1–4 exhibit a similar evolution to each other over the last 60 ka (Fig. 2). The main features are increases in dust% during HS 1–5, and these are strongest in Cores 2 and 3, which are positioned in the transition zone between dust and river dominated regions. There is also a gradual trend of increasing dust% from 60 ka to the LGM in Cores 1–3. In Cores 1 and 2, dust values decrease during the Bølling-Allerød (B-A; 14.7–12.9 ka) and increase during the Younger-Dryas (Y-D; 12.9–11.6 ka). In Cores 2 to 4, dust% values are lowest during the Holocene (Fig. 2c–e).

The interpolated latitudinal position of the sedimentary SSB (the 43 % ± 9 % dust value; Fig. 3c) follows a similar pattern to dust% values of the individual Cores 1–4. Over time, the SSB-dust value reaches its southernmost position (13° N ± 3°) during HS 1, 2, 4 and 5. It reaches 15° N ± 3° at the LGM and 16° N ± 3° during HS3. It reaches its northernmost position (21° N ± 5°) during the mid-Holocene and at ~ 51 ka (Fig. 3c).

5 Discussion

5.1 Controls on past sediment composition

The gradient in dust from 26° N to 3° N for the surface sediments and late Holocene section of the cores (Fig. 1c) suggests that the dust proportion reflects input from the adjacent continent (Figs. 1a, b). However, the absolute values of dust% from

Discussion Paper | Discussion Paper | Discussion Paper | Discussion Paper |

CPD

9, 119–142, 2013

Abrupt shifts of the Sahara-Sahel boundary

J. A. Collins et al.

sediments adjacent to the dust-dominated region appear rather low (e.g. 51 % at Core 1). Nonetheless, this value is comparable with estimates of dust% based on grain-size data (Tjallingii et al., 2008), suggesting it is not due to mis-characterisation of our dust and river end-members (Table S1 in the Supplement). Rather, because river-derived material is generally finer than dust (Gac and Kane, 1986), it is likely to be due to grain-size sorting processes. The low dust% values are hence thought to be due to lateral ocean advection and aggradation of the river end-member (Tjallingii et al., 2008). This suggests that sediments are slightly biased towards the river end-member, relative to the material exported from the adjacent continent.

Over time, however, changes in North–South ocean advection of fine river material are unlikely to be the main control on the past changes in dust versus river material in the sediment and on the position of the SSB. If this were the case, we would expect an anti-phase response at sites located within and to the north of the main river-sediment source. Instead, our cores positioned within (Cores 2–4) and to the north (Core 1) of the river-source regions display in-phase responses. The scatter between modern-day sediments (Fig. 1c) may be associated with local-scale controls on grain size such as sediment reworking, partitioning and winnowing. Over time, such changes may explain some of the small differences between the four records (Fig. 2b–e). However, the overall similarity of the 4 records suggests that a large-scale process must be the major control on the dust% evolution and on SSB position rather than local-scale sedimentation processes. The uncertainty on the modern-day SSB composition from the scatter in the modern-day surface samples (Fig. 1c) is transferred to our reconstruction of past SSB position. Finally, increased turbidite activity during HS could have contributed dune or dust-like material from the shelf and upper slope (Sarnthein and Diester-Haass, 1977; Hanebuth and Henrich, 2009; Henrich et al., 2010) and could have modified the composition of West African sediments. However, typical deep water benthic foraminiferal δ^{18}O values during HS from Core 2 (Mulitza et al., 2008), suggest autochthonous calcification and deposition rather than downslope transport from shallower and warmer water-masses. Thus, the increases in dust-like material during

CPD
9, 119–142, 2013

HS cannot have been delivered to the core site as turbidites originating from the upper slope, but rather as wind-blown dust.

The four cores are from a similar water depth (2278–3223 m) and so any grain size fractionation associated with transport distance should be similar between cores. In addition, the effect of sea-level changes (i.e. the core to shore distance) over time should be the same between cores. Moreover, although Just et al., (2012) suggest a control of sea level (i.e. increased proportion of river material during the glacial), we see no such control of sea level on dust% in our cores (Fig. 2).

Changes in wind direction might be expected to control the trajectory of the dust plume and thus could also control the latitudinal position of the sedimentary SSB. However, dune trends in Mauritania dated between 15–25 ka indicate a more zonal wind trajectory (NE–SW) compared to today (N–S; Lancaster et al., 2002). In fact, most relict dunes from other regions also display a (NE–SW) trajectory (Grove and Warren, 1968; Talbot, 1980). As such, the observed equatorward shifts of the sedimentary SSB during the glacial relative to today (Fig. 3c) cannot be attributed to a more meridional wind direction.

Therefore, we suggest that shifts in the sedimentary SSB are mainly due to shifts in position of the continental SSB. Strongest support for this comes from dune records, which indicate that sand dunes were forming as far south as $\sim 14^\circ$ N (Fig. 1a) in Senegal and Chad during glacial times (Grove, 1958; Michel, 1973; Servant, 1983), a similar latitude to the southernmost position of the sedimentary SSB (Fig. 3c).

Another important factor controlling both dust export and dune formation is wind strength (Sarnthein and Diester-Haass, 1977; Talbot, 1980). Wind strength was increased at the LGM (Sarnthein et al., 1981) and was very likely increased during other equatorward shifts of the SSB. For example, during HS, the grain size of the coarsest dust end-member of the sediment was increased (Mulitza et al., 2008), indicative of much stronger winds. In addition, Core 1 exhibits increased dust% during HS and the LGM even though it is positioned north of the SSB, and this is probably due to increased wind strength. This latter point also emphasises that the Sahara remained to the North of 21° N during HS: i.e. the entire latitudinal desert belt did not shift to the South during HS but rather the southern boundary shifted equatorwards, as has been also suggested for the LGM (Sarnthein et al., 1981). Although wind strength could have controlled the sedimentary SSB separately from the continental SSB, it cannot be the major control on the sedimentary SSB because of the latitudinal position of the continental dunes (see above).

5.2 Dune formation and dust mobilisation

The main episode of dune formation, when dunes reached 14° N, was the Ogolian phase, which has been dated at 15–24 ka in Mauritania (Lancaster et al., 2002), and slightly later 20–12 ka in Senegal (Michel, 1973) and Chad (Servant, 1983). The Ogolian phase is normally associated with LGM conditions (e.g. Talbot, 1980). Our data indicate that the sedimentary SSB was positioned at 15° N ± 3° at the LGM, (which is also in agreement with estimates from pollen-based studies; Dupont and Hooghiemstra, 1989; Lézine, 1989), and 13° N ± 3° at HS1. Considering that the glacial dust plume was stronger than today (Sarnthein et al., 1981), it is unlikely that the continental dunes could have reached 14° N while the sedimentary SSB was located further to the north (15° N). As such, we suggest that the southernmost dunes formed when the sedimentary SSB was at 13° N ± 3° rather than at 15° N ± 3°, i.e. at HS1 rather than the LGM. Morphological studies have suggested the path of the Senegal River was obstructed by shifting dunes during the Ogolian (Michel, 1973). Again, it seems likely that this took place, or was most severe, during HS1.

Another dune building phase at 14° N, the Early phase, has been dated at > 40 ka (Servant, 1983). During HS4 and HS5, the sedimentary SSB was also located at a latitude of 14° N ± 3° (Fig. 3c). This represents a shift of at least 7° ± 6° latitude from the background glacial state at this time. As such, rather than under background glacial conditions, dunes at 14° N were likely formed during HS4 and HS5.

What caused the equatorward shift of dunes and resultant increase in width of the dust plume? Sand dune formation and dust mobilisation can both be triggered by reduced vegetation cover, which is in turn due to reduced precipitation (Sarnthein and Diester-Haass, 1977; Prospero and Lamb, 2003). As such, an equatorward shifted SSB probably reflects a equatorward shift of the vegetation belts and this likely exposed new dust sources in the modern-day Sahel. Sand dunes do not normally act as dust sources, since they are too coarse, but they indicate persistence of sufficiently arid conditions for the mobilisation of dust. Although Sahelian dust sources are more chemically weathered than those in the Sahara (Stuut et al., 2005) this is still much less weathered than the river-derived end-member sourced from the Fouta Djallon (Gac and Kane, 1986; see also soil maps of Driessen et al., 2001). As well as dust mobilisation, precipitation amount also controls input of river sediment (Gac and Kane, 1986; Coynel et al., 2005). As such, reduced precipitation would simultaneously act to reduce input of the river end-member and increase input of the dust end-member.

Increased precipitation in arid regions could have potentially acted to increase input of "unweathered" material via river transport. However, it is unlikely that this coarse material would reach the core site: the coarser fraction is normally only be transported by wind. Moreover, hydrological proxies suggest drier conditions during HS (Niedermeyer et al., 2010), when our data display high dust% values.

5.3 Global climate teleconnections

The SSB exhibits a gradual equatorward shift from 60 ka to the LGM (Fig. 3c). This can be explained as a product of the gradual reduction in JAS cross-equatorial insolation gradient (Fig. 3a), as has been proposed for other studies (Zarriess et al., 2011). This would probably have decreased the SW wind strength and reduced the northward penetration of the summer monsoon, thus causing an equatorward shift of vegetation and the SSB. The gradual equatorward SSB shift may also be partly attributable to the increasing severity of glacial conditions from 60 ka to the LGM and the associated increases in aridity and wind strength. Conversely, during the mid-Holocene, increased JAS cross-equatorial insolation gradient induced greater northward penetration of the

West African monsoon (Kutzbach and Liu, 1997), increasing vegetation coverage in the Sahel and Sahara (e.g. Salzmann and Waller, 1998; Watrin et al., 2009). Our dust estimate of SSB position during the mid-Holocene (21° N ± 3°) is in broad agreement with estimates determined from plant community distribution (23° N; Watrin et al., 2009). The increase in dust% from the mid to late Holocene (Figs. 2b–e, 3c), was relatively minor compared to the rest of our record. This is in line with dune records suggesting that the Late phase of sand dune formation (Fig. 3) was associated with relatively minor mobilisation of sand (Talbot, 1980). Lastly, none of our records display an abrupt increase in dust from the mid to late Holocene (Figs. 2b–e, 3c) as seen in another record (deMenocal et al., 2000). Our data thus suggest a gradual response to insolation forcing.

The abrupt changes in SSB position appear to be the result of a sharp decrease in North Atlantic sea surface temperatures (SSTs). The North Atlantic and particularly the Iberian Margin (Figs. 2a, 3b) underwent extreme cooling during HS (e.g. Cortijo et al., 1997; de Abreu et al., 2003; Martrat et al., 2007; Eynaud et al., 2009; Kageyama et al., 2009; Salgueiro et al., 2010). This cooling is thought to have been due to slowdown of the AMOC and reduced deepwater production during HS (e.g. McManus et al., 2004). The cooling is manifested as equatorward shifts of the polar front as far South as the Iberian Margin (Eynaud et al., 2009). The magnitude of SST changes during HS appears to be closely coupled to shifts of the SSB. For example, the coolest SSTs (HS1, HS4 and HS5; Fig. 3b) and thus the most intense equatorward shifts of the polar front (Eynaud et al., 2009) resulted in the largest equatorward SSB shifts (Fig. 3c). HS2 is slightly anomalous in this regard (most records show small magnitude cooling) although there is a larger cooling at HS2 in Cortijo et al. (1997). Also, in the record from Martrat et al. (2007), HS4 is anomalously cool compared to other records. The coupling between dust and SST is also seen within HS: the three-phase evolution of HS (Bouimetarhan et al., 2012) appears to be visible in both the SST (Fig. 2a) and dust% (Fig. 2b) during HS1 and HS2.

CPD
9, 119–142, 2013

SST is linked to the SSB position via its control on precipitation and wind strength. The marked cooling in the North Atlantic is thought to have increased the strength of the African Easterly Jet which led to reduced precipitation in the Sahel (Mulitza et al., 2008; Bouimetarhan et al., 2012) and would have caused the aforementioned equatorward shift of vegetation zones. Trade-wind strength, on the other hand, is thought to be controlled by the meridional SST gradient (e.g. Kim et al., 2003). Therefore, we suggest that the SST difference between the Iberian Margin (Martrat et al., 2007) and the Gulf of Guinea (Weldeab et al., 2007), which was greater by up to 4 °C during HS (Fig. 3d), acted to increase the strength of the NE trade winds and thus the "strength" of the dust plume. This mechanism may explain why increases in dust input and grain size are so strong during HS.

The SSB position was shifted equatorward to 17° N ± 2° at the Y-D (Fig. 3c) which is in line with increased dune activity in Mauritania at ~ 19° N at this time (Lancaster et al., 2002). In most records, there is a relatively small SST decrease in the NE Atlantic (Fig. 2a), although cooling in the northern high latitudes was relatively large (Fig. 2f). This therefore suggests a different mechanism of transmission compared to HS, perhaps via an atmospheric teleconnection.

The response of the position of the SSB to changes in SST was rapid, both equatorward and poleward (Fig. 3c). All cores responded coevally indicating a very rapid expansion and retreat of the SSB. At HS5 for example, the SSB migrated 7° south and 7° north in 4 ka, equivalent to a rate of approximately 400 $\mathrm{m\,yr^{-1}}$ (Fig. 3c). This is at least an order of magnitude greater than modern estimates of dune migration rate: 7.5 $\mathrm{m\,yr^{-1}}$ for barchan dunes in NW Sudan (Haynes Jr, 1989) and between 0.17 and 30 $\mathrm{m\,yr^{-1}}$ for other regions (Marín et al., 2005; Bristow et al., 2005; Muckersie and Shepherd, 1995). The speed of dune migration highlights the potential for dune re-activation and increased dust export during a future precipitation decrease in the Western Sahel (Meehl et al., 2007).

Finally, the latitudinal expansion of the dust plume by 6° during HS1, 2, 4 and 5 relative to today, combined with increased plume strength would have increased global

CPD
9, 119–142, 2013

atmospheric dust loading. The magnitude of feedbacks from such an increase in atmospheric dust loading requires further investigation, in particular regarding its contribution to the cooling (Miller and Tegen, 1998) and aridity (Rosenfeld et al., 2001) of Heinrich Stadials.

6 Conclusions

We have presented a high-resolution record of the position of the Sahara-Sahel Boundary (SSB) over the last 60 ka based on the dust% in hemipelagic sediments retrieved from a latitudinal transect off West Africa. Our data indicate that sediments composed of 43 % ± 9 % dust, equivalent to those at the modern-day SSB (19° N), were present down to a latitude of 13° N ± 3° during HS1, 2, 4 and 5. This represents an equatorward shift of around 6° relative to the modern-day. Evidence for relict sand dunes at 14° N latitude on the continent supports our interpretation that the sediments reflect shifts of the continental SSB. We find that the largest and most abrupt equatorward shifts of the SSB position were likely induced by extremely cold North Atlantic sea surface temperatures during Heinrich Stadials.

Supplementary material related to this article is available online at: http://www.clim-past-discuss.net/9/119/2013/cpd-9-119-2013-supplement.pdf.

Acknowledgements. This work was supported by ESF-EUROMARC project "RETRO", the DFG Research Centre/Cluster of Excellence MARUM "The Ocean in the Earth System", the Helmholtz Climate Initiative "REKLIM" and GLOMAR – Bremen International Graduate School for Marine Sciences. We acknowledge Vera Lukies and Karsten Enneking for analytical assistance during XRF scanning and powder analysis. Sample material has been provided by the GeoB Core Repository at the MARUM – Center for Marine Environmental Sciences, University of Bremen, Germany. The data reported in this paper are archived in the Pangaea database (www.pangaea.de).

CPD
9, 119–142, 2013

References

Bory, A. J. M. and Newton, P. P.: Transport of airborne lithogenic material down through the water column in two contrasting regions of the eastern subtropical North Atlantic Ocean, Global Biogeochem. Cy., 14, 297–315, 2000.

Bouimetarhan, I., Prange, M., Schefuß, E., Dupont, L., Lippold, J., Mulitza, S., and Zonneveld, K.: Sahel megadrought during Heinrich stadial 1: evidence for a three-phase evolution of the low- and mid-level West African wind system, Quaternary Sci. Rev., 58, 66–76, 2012.

Bristow, C. S., Lancaster, N., and Duller, G. A. T.: Combining ground penetrating radar surveys and optical dating to determine dune migration in Namibia, J. Geol. Soc., 162, 315–321, 2005.

Castañeda, I. S., Mulitza, S., Schefuß, E., Lopes dos Santos, R. A., Sinninghe Damsté, J. S., and Schouten, S.: Wet phases in the Sahara/Sahel region and human migration patterns in North Africa, P. Natl. Acad. Sci. USA, 106, 20159–20163, 2009.

Collins, J. A., Schefuß, E., Heslop, D., Mulitza, S., Prange, M., Zabel, M., Tjallingii, R., Dokken, T. M., Huang, E., Mackensen, A., Schulz, M., Tian, J., Zarriess, M., and Wefer, G.: Interhemispheric symmetry of the tropical African rainbelt over the past 23 000 years, Nat. Geosci., 4, 42–45, 2011.

Cortijo, E., Labeyrie, L., Vidal, L., Vautravers, M., Chapman, M., Duplessy, J.-C., Elliot, M., Arnold, M., Turon, J.-L., and Auffret, G.: Changes in sea surface hydrology associated with Heinrich event 4 in the North Atlantic Ocean between 40° and 60° N, Earth Planet. Sc. Lett., 146, 29–45, 1997.

Coynel, A., Seyler, P., Etcheber, H., Meybeck, M., and Orange, D.: Spatial and seasonal dynamics of total suspended sediment and organic carbon species in the Congo River, Global Biogeochem. Cy., 19, GB4019, doi:10.1029/2004GB002335, 2005.

de Abreu, L., Shackleton, N. J., Schönfeld, J., Hall, M., and Chapman, M.: Millennial-scale oceanic climate variability off the Western Iberian margin during the last two glacial periods, Mar. Geol., 196, 1–20, 2003.

deMenocal, P. B.: Plio-Pleistocene African climate, Science, 270, 53–59, 1995.

deMenocal, P., Ortiz, J., Guilderson, T., Adkins, J., Sarnthein, M., Baker, L., and Yarusinsky, M.: Abrupt onset and termination of the African Humid Period: rapid climate responses to gradual insolation forcing, Quaternary Sci. Rev., 19, 347–361, 2000.

Driessen, P. M., Deckers, J. A., Spaargaren, O. C., and Nachtergaele, F. O.: Lecture Notes on the Major Soils of the World, Food and Agriculture Organization of the United Nations, Rome, 2001.
Dupont, L. M. and Hooghiemstra, H.: The Saharan-Sahelian boundary during the Brunhes chron., Acta Bot. Neerl., 38, 405–415, 1989.
Eynaud, F., de Abreu, L., Voelker, A., Schönfeld, J., Salgueiro, E., Turon, J.-L., Penaud, A., Toucanne, S., Naughton, F., Sánchez Goñi, M. F., Malaizé, B., and Cacho, I.: Position of the Polar Front along the western Iberian margin during key cold episodes of the last 45 ka, Geochem. Geophys. Geosys., 10, Q07U05, doi:10.1029/2009GC002398, 2009.
FAO, Fighting sand enroachment: lessons from Mauritania, FAO Forestry Paper 158, Rome, 2010.
Gac, J. Y. and Kane, A.: Le fleuve Sénégal: I, Bilan hydrologique et flux continentaux de matières particulaires à l'embouchure, Sci. Géol. Bull., 39, 99–130, 1986.
Goudie, A. S. and Middleton, N. J.: Saharan dust storms: nature and consequences, Earth-Sci. Rev., 56, 179–204, 2001.
Govin, A., Holzwarth, U., Heslop, D., Ford Keeling, L., Zabel, M., Mulitza, S., Collins, J. A., and Chiessi, C. M.: Distribution of major elements in Atlantic surface sediments (36° N–49° S): imprint of terrigenous input and continental weathering, Geochem. Geophys. Geosys., 13, Q01013, doi:10.1029/2011GC003785, 2012.
Govin, A., Collins, J. A., Heslop, D., Zabel, M., Mulitza, S., and Röhl, U.: History of Western African precipitation (21° N–20° S) during the last 145 ka: orbital- versus millennial-scale variability, submitted, 2013.
Grousset, F. E., Parra, M., Bory, A., Martinez, P., Bertrand, P., Shimmield, G., and Ellam, R. M.: Saharan wind regimes traced by the Sr-Nd isotopic composition of subtropical Atlantic sediments: Last Glacial Maximum vs today, Quaternary Sci. Rev., 17, 395–409, 1998.
Grove, A. T.: The ancient erg of Hausaland, and similar formations on the south side of the Sahara, Geogr. J., 124, 528–533, 1958.
Grove, A. T. and Warren, A.: Quaternary landforms and climate on the south side of the Sahara, Geogr. J., 134, 194–208, 1968.
Hanebuth, T. J. J. and Henrich, R.: Recurrent decadal-scale dust events over Holocene western Africa and their control on canyon turbidite activity (Mauritania), Quaternary Sci. Rev., 28, 261–270, 2009.

Haynes Jr., C. V.: Bagnold's barchan: a 57-yr record of dune movement in the eastern Sahara and implications for dune origin and paleoclimate since Neolithic times, Quaternary Res., 32, 153–167, 1989.

Henrich, R., Cherubini, Y., and Meggers, H.: Climate and sea level induced turbidite activity in a canyon system offshore the hyperarid Western Sahara (Mauritania): the Timiris Canyon, Mar. Geol., 275, 178–198, 2010.

Hooghiemstra, H., Lézine, A.-M., Leroy, S. A. G., Dupont, L., and Marret, F.: Late Quaternary palynology in marine sediments: a synthesis of the understanding of pollen distribution patterns in the NW African setting, Quat. Internat., 148, 29–44, 2006.

Itambi, A. C., von Dobeneck, T., Mulitza, S., Bickert, T., and Heslop, D.: Millennial-scale northwest African droughts related to Heinrich events and Dansgaard-Oeschger cycles: evidence in marine sediments from offshore Senegal, Paleoceanography, 24, PA1205, doi:10.1029/2007PA001570, 2009.

Jullien, E., Grousset, F., Malaizé, B., Duprat, J., Sanchez-Goni, M. F., Eynaud, F., Charlier, K., Schneider, R., Bory, A., Bout, V., and Flores, J. A.: Low-latitude "dusty events" vs. high-latitude "icy Heinrich events", Quaternary Res., 68, 379–386, 2007.

Just, J., Heslop, D., von Dobeneck, T., Bickert, T., Dekkers, M. J., Frederichs, T., Meyer, I., and Zabel, M.: Multiproxy characterization and budgeting of terrigenous end-members at the NW African continental margin, Geochem. Geophys. Geosyst., 13, Q0AO01, doi:10.1029/2012GC004148, 2012.

Kageyama, M., Mignot, J., Swingedouw, D., Marzin, C., Alkama, R., and Marti, O.: Glacial climate sensitivity to different states of the Atlantic Meridional Overturning Circulation: results from the IPSL model, Clim. Past, 5, 551–570, doi:10.5194/cp-5-551-2009, 2009.

Kim, J.-H., Schneider, R. R., Mulitza, S., and Muller, P. J.: Reconstruction of SE trade-wind intensity based on sea-surface temperature gradients in the Southeast Atlantic over the last 25 kyr, Geophys. Res. Lett., 30, 2144, doi:10.1029/2003GL017557, 2003.

Kocurek, G., Havholm, K. G., Deynoux, M. A. X., and Blakey, R. C.: Amalgamated accumulations resulting from climatic and eustatic changes, Akchar Erg, Mauritania, Sedimentology, 38, 751–772, 1991.

Kutzbach, J. E. and Liu, Z.: Response of the African monsoon to orbital forcing and ocean feedbacks in the middle Holocene, Science, 278, 440–443, 1997.

CPD
9, 119–142, 2013

Lancaster, N., Kocurek, G., Singhvi, A., Pandey, V., Deynoux, M., Ghienne, J.-F., and Lo, K.: Late Pleistocene and Holocene dune activity and wind regimes in the western Sahara Desert of Mauritania, Geology, 30, 991–994, 2002.

Lézine, A.-M.: Late quaternary vegetation and climate of the Sahel, Quaternary Res., 32, 317–334, 1989.

Mahowald, N. M., Baker, A. R., Bergametti, G., Brooks, N., Duce, R. A., Jickells, T. D., Kubilay, N., Prospero, J. M., and Tegen, I.: Atmospheric global dust cycle and iron inputs to the ocean, Global Biogeochem. Cy., 19, GB4025, doi:10.1029/2004GB002402, 2005.

Marín, L., Forman, S. L., Valdez, A., and Bunch, F.: Twentieth century dune migration at the Great Sand Dunes National Park and Preserve, Colorado, relation to drought variability, Geomorphology, 70, 163–183, 2005.

Martrat, B., Grimalt, J. O., Shackleton, N. J., de Abreu, L., Hutterli, M. A., and Stocker, T. F.: Four climate cycles of recurring deep and surface water destabilizations on the Iberian margin, Science, 317, 502–507, 2007.

McManus, J. F., Francois, R., Gherardi, J. M., Keigwin, L. D., and Brown-Leger, S.: Collapse and rapid resumption of Atlantic meridional circulation linked to deglacial climate changes, Nature, 428, 834–837, 2004.

Meehl, G. A., Stocker, T. F., Collins, W. D., Friedlingstein, P., Gaye, A. T., Gregory, J. M., Kitoh, A., Knutti, R., Murphy, J. M., Noda, A., Raper, S. C. B., Watterson, I. G., Weaver, A. J., and Zhao, Z.-C.: Global Climate Projections, in: Climate Change 2007: the Physical Science Basis, Contribution of Working Group I to the Fourth Assessment Report of the Intergovernmental Panel on Climate Change, edited by: Solomon, S., Qin, D., Manning, M., Chen, Z., Marquis, M., Averyt, K. B., Tignor, M., and Miller, H. L., Cambridge University Press, Cambridge, UK and New York, NY, USA, 2007.

Michel, P.: Les bassins des fleuves Sénégal et Gambie, Etude géomorphologique, ORSTROM, Paris, 1973.

Miller, R. L. and Tegen, I.: Climate response to soil dust aerosols, J. Climate, 11, 3247–3267, 1998.

Muckersie, C. and Shepherd, M. J.: Dune phases as time-transgressive phenomena, Manawatu, New Zealand, Quat. Internat., 26, 61–67, 1995.

Mulitza, S., Prange, M., Stuut, J. B., Zabel, M., von Dobeneck, T., Itambi, A. C., Nizou, J., Schulz, M., and Wefer, G.: Sahel megadroughts triggered by glacial slowdowns of Atlantic meridional overturning, Paleoceanography, 23, PA4206, doi:10.1029/2008PA001637, 2008.

NGRIP: High-resolution record of Northern Hemisphere climate extending into the last interglacial period, Nature, 431, 147–151, 2004.
Niedermeyer, E. M., Schefuß, E., Sessions, A. L., Mulitza, S., Mollenhauer, G., Schulz, M., and Wefer, G.: Orbital- and millennial-scale changes in the hydrologic cycle and vegetation in the western African Sahel: insights from individual plant wax δD and δ^{13}C, Quaternary Sci. Rev., 29, 2996–3005, 2010.
Prospero, J. M. and Lamb, P. J.: African droughts and dust transport to the Caribbean: climate change implications, Science, 302, 1024–1027, 2003.
Prospero, J. M., Glaccum, R. A., and Nees, R. T.: Atmospheric transport of soil dust from Africa to South America, Nature, 289, 570–572, 1981.
Rosenfeld, D., Rudich, Y., and Lahav, R.: Desert dust suppressing precipitation: a possible desertification feedback loop, P. Natl. Acad. Sci. USA, 98, 5975–5980, 2001.
Salgueiro, E., Voelker, A. H. L., de Abreu, L., Abrantes, F., Meggers, H., and Wefer, G.: Temperature and productivity changes off the western Iberian margin during the last 150 ky, Quaternary Sci. Rev., 29, 680–695, 2010.
Salzmann, U. and Waller, M.: The Holocene vegetational history of the Nigerian Sahel based on multiple pollen profiles, Rev. Palaeobot. Palyno., 100, 39–72, 1998.
Sarnthein, M. and Diester-Haass, L.: Eolian-sand turbidites, J. Sediment. Res., 47, 868–890, 1977.
Sarnthein, M., Tetzlaff, G., Koopmann, B., Wolter, K., and Pflaumann, U.: Glacial and interglacial wind regimes over the eastern subtropical Atlantic and North-West Africa, Nature, 293, 193–196, 1981.
Servant, M.: Séquences continentales et variations climatiques: évolution du bassin du Tchad au Cénozoique supérieur, Travaux et Documents de l'ORSTOM, 159, 1983.
Stuut, J.-B., Zabel, M., Ratmeyer, V., Helmke, P., Schefuß, E., Lavik, G., and Schneider, R.: Provenance of present-day eolian dust collected off NW Africa, J. Geophys. Res., 110, D04202, doi:10.1029/2004JD005161, 2005.
Svensson, A., Andersen, K. K., Bigler, M., Clausen, H. B., Dahl-Jensen, D., Davies, S. M., Johnsen, S. J., Muscheler, R., Parrenin, F., Rasmussen, S. O., Röthlisberger, R., Seierstad, I., Steffensen, J. P., and Vinther, B. M.: A 60 000 year Greenland stratigraphic ice core chronology, Clim. Past, 4, 47–57, doi:10.5194/cp-4-47-2008, 2008.
Swezey, C.: Eolian sediment responses to late Quaternary climate changes: temporal and spatial patterns in the Sahara, Palaeogeogr. Palaeocl., 167, 119–155, 2001.

Discussion Paper | Discussion Paper | Discussion Paper | Discussion Paper |

Talbot, M. R.: Environmental responses to climatic change in the West African Sahel over the past 20 000 years, in: The Sahara and the Nile, Quaternary environments and prehistoric occupation in northern Africa, edited by: Williams, M. A. J. and Faure, H., A. A. Balkema, Rotterdam, 37–62, 1980.
Tjallingii, R., Claussen, M., Stuut, J.-B. W., Fohlmeister, J., Jahn, A., Bickert, T., Lamy, F., and Rohl, U.: Coherent high- and low-latitude control of the northwest African hydrological balance, Nat. Geosci., 1, 670–675, 2008.
Watrin, J., Lézine, A.-M., and Hély, C.: Plant migration and plant communities at the time of the "green Sahara", C. R. Geosci., 341, 656–670, 2009.
Weldeab, S., Lea, D. W., Schneider, R. R., and Andersen, N.: 155 000 years of West African monsoon and ocean thermal evolution, Science, 316, 1303–1307, 2007.
Weltje, G. J. and Tjallingii, R.: Calibration of XRF core scanners for quantitative geochemical logging of sediment cores: theory and application, Earth Planet. Sc. Lett., 274, 423–438, 2008.
Zarriess, M. and Mackensen, A.: The tropical rainbelt and productivity changes off northwest Africa: a 31 000-year high-resolution record, Mar. Micropaleontol., 76, 76–91, 2010.
Zarriess, M., Johnstone, H., Prange, M., Steph, S., Groeneveld, J., Mulitza, S., and Mackensen, A.: Bipolar seesaw in the northeastern tropical Atlantic during Heinrich stadials, Geophys. Res. Lett., 38, L04706, doi:10.1029/2010GL046070, 2011.

CPD
9, 119–142, 2013

Table 1. Sediment core transect.

Core Label	Core Number	Latitude	Longitude	Water Depth (m)	Age model based on	Age model reference
1	GeoB7920-2	20°45.09′ N	18° 34.90′ W	2278	^{14}C, $\delta^{18}O$	Tjallingii et al. (2008); Collins et al. (2011)
2	GeoB9508-5	15°29.90′ N	17° 56.88′ W	2384	^{14}C, $\delta^{18}O$	Mulitza et al. (2008)
3	GeoB9526-5	12°26.10′ N	18° 03.40′ W	3223	^{14}C, $\delta^{18}O$	Zarriess and Mackensen (2010); Zarriess et al. (2011)
4	GeoB9528-3	09°09.96′ N	17° 39.81′ W	3057	$\delta^{18}O$	Castañeda et al. (2009); Govin et al. (2013)

CPD
9, 119–142, 2013

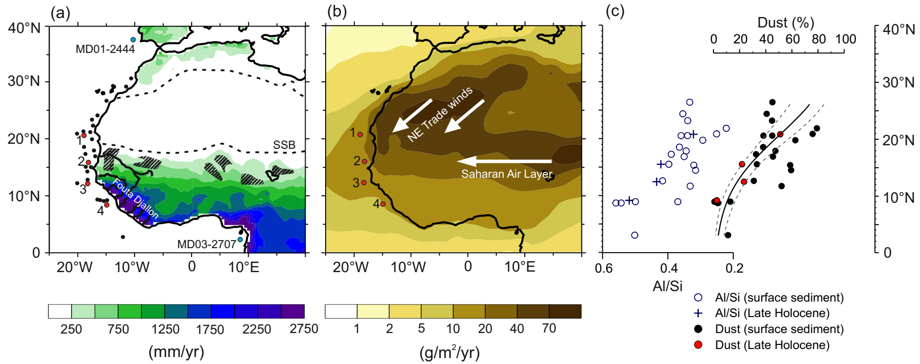

Fig. 1. (a) Annual-mean rainfall (mm yr^{-1}) for West Africa from the University of Delaware precipitation dataset (http://climate.geog.udel.edu/~climate; average for 1950–1999). Thick black lines highlight the main African rivers of the study area: the Senegal River, Gambia River as well as numerous small rivers in Guinea, Sierra Leone and Liberia. Hatching marks the position of relict sand dunes in the Sahel, re-drawn after Grove (1958). Black dotted lines mark the approximate boundaries of modern-day dune formation (Sarnthein and Diester-Haass, 1977). Red dots mark locations of Cores 1–4 (see Table 1). Blue dots mark the locations of cores MD01-2444 (Martrat et al., 2007) and MD03-2707 (Weldeab et al., 2007). Black dots mark locations of surface samples plotted in Fig. 1c (Govin et al., 2012). **(b)** Modern-day dust deposition (g m^{-2} yr^{-1}) for West Africa (Mahowald et al., 2005), highlighting the Saharan dust plume. **(c)** Al/Si (blue; axis inverted) and dust% (black and red) of surface sediments (Govin et al., 2012) and late Holocene section of Cores 1–4. Solid line represents robust linear regression between latitude and dust% (plot is rotated 90°) for samples covering the gradient between dust and river material (26° N–3° N). Data have been transformed as log((100 – dust%)/dust%) so that the regression lies in the interval (0, 100). The correlation (r^2) is 0.51. Dotted lines represent 68 % confidence intervals, which equates to on average plus/minus 9 % dust.

CPD
9, 119–142, 2013

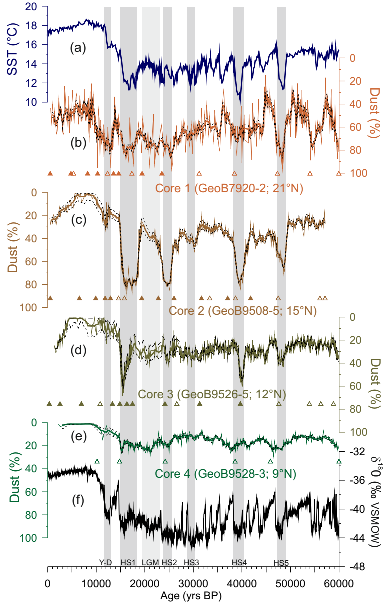

Fig. 2. Records of dust% from the West African margin compared with NE Atlantic SST and Greenland Ice Core δ^{18}O. **(a)** SST of the Iberian Margin (Core MD01-2444; 38° N; Martrat et al., 2007). **(b)–(e)** Dust% for Core 1 (GeoB7920-2, 21° N), Core 2 (GeoB9508-5; 15° N), Core 3 (GeoB9526-5; 12° N) and Core 4 (GeoB9528-3; 9° N). Note that y-axes are inverted. Solid line is the median of 500 iterations. Thick line represents a 5 point running average. Uncertainty (black dashed lines) includes: uncertainty on end-member composition (based on 16th and 84th percentiles of 500 iterations) and uncertainty on marine component (based on variations in opal content). Grey bars highlight Heinrich Stadials. Timing is based on the D-O stadials in Greenland ice (Fig. 2f; Svensson et al., 2008). **(f)** δ^{18}O of Greenland ice (NGRIP, 2004, Svensson et al., 2008; 5 point running average). Filled triangles indicate AMS radiocarbon ages. Open triangles indicate tie-points derived from benthic foraminiferal δ^{18}O correlation (see Table 1 for references).

CPD
9, 119–142, 2013

Abrupt shifts of the Sahara-Sahel boundary

J. A. Collins et al.

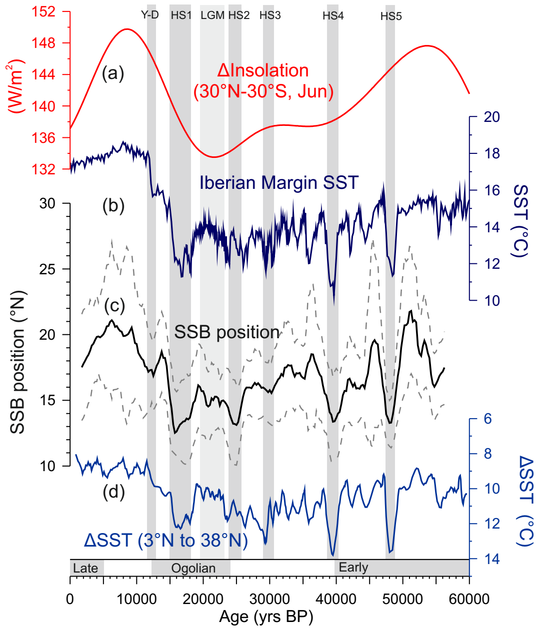

Fig. 3. **(a)** Boreal summer (JAS) insolation gradient between 30° N and 30° S. **(b)** SST of the Iberian Margin (Martrat et al., 2007). **(c)** Latitudinal position of the sedimentary SSB (43 % dust value) over the last 60 ka. Thick line represents the five-point running average. Uncertainty (grey dashed lines) includes: uncertainty on the end-member compositions (as in Fig. 2), uncertainty on modern-day dust% at the SSB (based on 68 % confidence intervals; Fig. 1c) and uncertainty on the regression for past timesteps (68 % confidence intervals; examples are given in Fig. SF3). **(d)** SST difference (5 point running average) between the Iberian Margin (MD01-2444; 38° N; Martrat et al., 2007) and the Gulf of Guinea (MD03-2707: 3° N; Weldeab et al., 2007). Vertical grey bars highlight HS, YD and LGM. The Early, Ogolian and Late phases of dune formation are marked.

CPD
9, 119–142, 2013